

Magnetic properties of the self-doped yttrium manganites $\text{YMn}_{1+x}\text{O}_3$

This article has been downloaded from IOPscience. Please scroll down to see the full text article.

2005 J. Phys.: Condens. Matter 17 8029

(<http://iopscience.iop.org/0953-8984/17/50/020>)

View [the table of contents for this issue](#), or go to the [journal homepage](#) for more

Download details:

IP Address: 129.252.86.83

The article was downloaded on 28/05/2010 at 07:09

Please note that [terms and conditions apply](#).

Magnetic properties of the self-doped yttrium manganites $\text{YMn}_{1+x}\text{O}_3$

W R Chen, F C Zhang, J Miao, B Xu, L X Cao, X G Qiu and B R Zhao¹

Laboratory for Superconductivity, Institute of Physics and Center for Condensed Matter Physics, Chinese Academy of Sciences, PO Box 603, Beijing 100080, People's Republic of China

E-mail: brzhao@aphy.iphy.ac.cn

Received 10 August 2005, in final form 13 October 2005

Published 2 December 2005

Online at stacks.iop.org/JPhysCM/17/8029

Abstract

Magnetic properties of the hexagonal compounds of $\text{YMn}_{1+x}\text{O}_3$ ($0 \leq x \leq 0.15$) have been studied by measuring the dc magnetization, ac magnetization, magnetic hysteresis, and relaxation of the magnetization. All the results give evidence of a spin glass (SG) state at low temperatures in samples with $x \geq 0.08$. This is attributed to the competition between the antiferromagnetic (AFM) matrix and the ferromagnetic (FM) phase induced by the excess Mn. Moreover, careful investigations on the thermoremanent magnetization (TRM) of the sample with $x = 0.10$ indicate that this SG state is an ideal state with nearly infinite equilibration time and that it shows almost perfect full ageing.

1. Introduction

Over the past few years, a large amount of research has been carried out towards understanding the physical properties of $\text{R}_{1-x}\text{A}_x\text{MnO}_3$, with R as a rare-earth or yttrium and A as an alkaline-earth ion. For large and small rare-earth ions, RMnO_3 crystallizes into orthorhombic and hexagonal structures, respectively. Manganites both of a perovskite and of a hexagonal structure are fascinating materials displaying a variety of interesting properties, like colossal magnetoresistance or ferroelectricity, which are strongly affected by the stoichiometry of the studied samples. For materials with orthorhombic structure, the ground state of the parent compound RMnO_3 is of long-range antiferromagnetic (AFM) order. For doped compound $\text{R}_{1-x}\text{A}_x\text{MnO}_3$ ($\text{A} = \text{Ca}, \text{Sr}, \text{Ba}$), with x in the range 0.22–0.50, the system has a ferromagnetic (FM) state owing to the double-exchange interaction [1]. One can also make materials, for example, $(\text{Tb-La})_{0.67}\text{Ca}_{0.33}\text{MnO}_3$ [2], $(\text{La-Dy})_{0.7}\text{Ca}_{0.3}\text{MnO}_3$ [3] and $\text{La}_{0.46}\text{Sr}_{0.54}\text{Mn}_{0.98}\text{Cr}_{0.02}\text{O}_3$ [4], that have spin glass (SG) as the low-temperature ground state due to the competition between the FM double-exchange interaction and the AFM superexchange interaction.

¹ Author to whom any correspondence should be addressed.

In comparison with perovskites, the investigation on the doping effect on hexagonal manganites is very sparse. YMnO_3 [5–7], one of the most studied hexagonal manganites, has an A-type AFM structure. The spins on Mn ions within the Mn–O plane form a triangular network and two neighbouring Mn ions share the other Mn ion as their nearest neighbour. Since it is impossible to satisfy all nearest-neighbour AFM coupling, the system forms a geometrically frustrated magnetic state. In order to modify the AFM interaction, the traditional method to replace the Y^{3+} partially by cations such as Ca^{2+} or Sr^{2+} was unsuccessful [8, 9], because a small concentration of doped Ca or Sr would bring about an orthorhombic impurity phase in the hexagonal structure. Another way of self-doping manganite has recently been reported to effectively modify the magnetic interaction, as well as maintain the single hexagonal phase [10]. Mn-rich $\text{YMn}_{1.10}\text{O}_3$ shows a reentrant SG state at low temperatures, in which the geometric magnetic frustration plays an important role. In this paper we report detailed studies on the magnetic properties of the self-doped series of $\text{YMn}_{1+x}\text{O}_3$ in the range $0 \leq x \leq 0.15$.

2. Experimental details

Polycrystalline samples of different compositions of $\text{YMn}_{1+x}\text{O}_3$ ($0 \leq x \leq 0.15$) were prepared by the conventional solid-state reaction method. Mixed high-purity Y_2O_3 and MnO_2 powders for each sample were calcined twice at 900°C for 12 h. The powders were sintered at 1450°C for several days with intermittent grindings to ensure complete reaction. They were then subsequently pulverized, compressed and sintered at 1450°C for 12 h to achieve improved compactness. The step x-ray diffraction analysis results indicate that all the samples are pure with a single hexagonal phase. The dc magnetic susceptibility χ_{dc} , the hysteresis $M(H)$, the relaxation of magnetization $M(t)$ and the thermoremanent magnetization (TRM) were measured with a superconducting quantum interference device magnetometer. The ac magnetic susceptibility measurement was carried out with a physical property measuring system.

3. Results and discussion

The temperature dependence of the dc magnetic susceptibility χ_{dc} was measured in an applied field of 100 Oe for $\text{YMn}_{1+x}\text{O}_3$ samples ($x = 0, 0.05, 0.08, 0.10, 0.12$ and 0.15). We show a typical four representative samples ($x = 0.05, 0.08, 0.10$, and 0.15) in figure 1. There is no anomaly observed in the dc magnetization for the $x = 0.05$ sample, which is similar to the parent compound YMnO_3 [5–7]. As regards the $x = 0.08$ sample, however, the magnetization increases sharply when the temperature is decreased to about 39 K. This indicates that when the excess content of Mn increases to 0.08, a magnetic phase transition occurs. The temperature dependence dc magnetization for all specimens was taken under zero-field-cooled (ZFC) and field-cooled (FC) conditions by applying various magnetic fields. The data for the sample with $x = 0.10$ in magnetic fields of 0.01, 0.3 and 5 T are presented in figure 2. A cusp in the ZFC curve at 42 K and a distinctive separation of the ZFC and FC curves below that temperature are consistent with an SG phase at 42 K. It is also found that the sharp maximum in the ZFC curve becomes smeared out and shifts to a lower temperature with increasing external fields. On the other hand, at a given temperature and in the field range from 100 Oe to 5 T the magnetization increases monotonically but no maximum is reached. Similar dc magnetization behaviours were also observed for the other specimens with $x = 0.08, 0.12$ and 0.15 .

By fitting the inverse susceptibility $1/\chi_{\text{dc}}$ to the Curie–Weiss law $\chi = C/(T - \theta_{\text{CW}})$, we obtain the Curie–Weiss temperature θ_{CW} and the effective moment μ_{J} for all the samples, which are shown in table 1. The parent compound YMnO_3 has a Curie–Weiss temperature

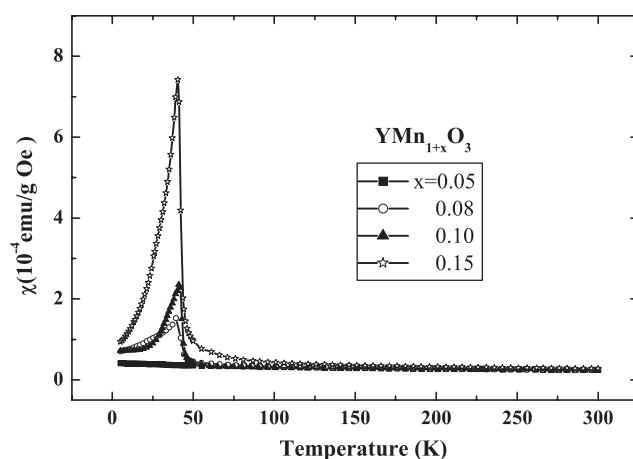


Figure 1. Temperature dependence of the dc magnetic susceptibility χ_{dc} at $H = 100$ Oe under the zero-field-cooled (ZFC) condition for four typical $\text{YMn}_{1+x}\text{O}_3$ samples ($x = 0.05, 0.08, 0.10,$ and 0.15).

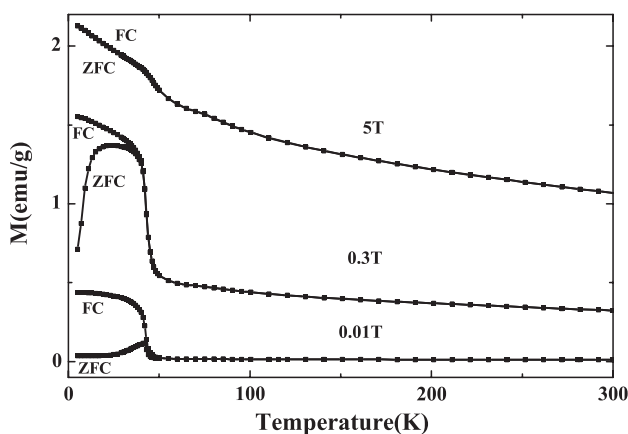


Figure 2. Temperature dependence of the FC and ZFC magnetization for $x = 0.10$ sample at 0.01, 0.3, and 5 T. To plot the curves in the same scale, we have multiplied both the 0.01 T and the 0.3 T data by the factor 5.

$\theta_{CW} = -330$ K and an effective moment $\mu_J = 4.70 \mu_B$. The value of the effective moment μ_J for YMnO_3 is smaller than that expected for Mn^{3+} , $4.90 \mu_B$, which is also reported in the previous study [11]. When the excess Mn is introduced into YMnO_3 , both $|\theta_{CW}|$ and μ_J are increased. Since θ_{CW} is a measure of the AFM coupling strength between Mn ions, the result suggests that the Mn doping enhances the AFM interaction, in contrast to most AFM compounds where impurities usually suppress the AFM interaction. We note, however, that the substitution of Cd for Zn in the spinel $\text{Zn}_{1-x}\text{Cd}_x\text{Cr}_2\text{O}_4$ ($x = 0.05, 0.10$) [12] also enhances the AFM interaction and drives the system from a frustrated antiferromagnet to an SG state in the low-temperature region. In addition, the values of μ_J indicate that Mn doping may result in a mixed valence state of Mn^{2+} and Mn^{3+} in Mn-rich YMnO_3 .

In order to obtain more information on the magnetic state of the Mn-rich $\text{YMn}_{1+x}\text{O}_3$ system, we performed frequency-dependent susceptibility measurements at an ac magnetic

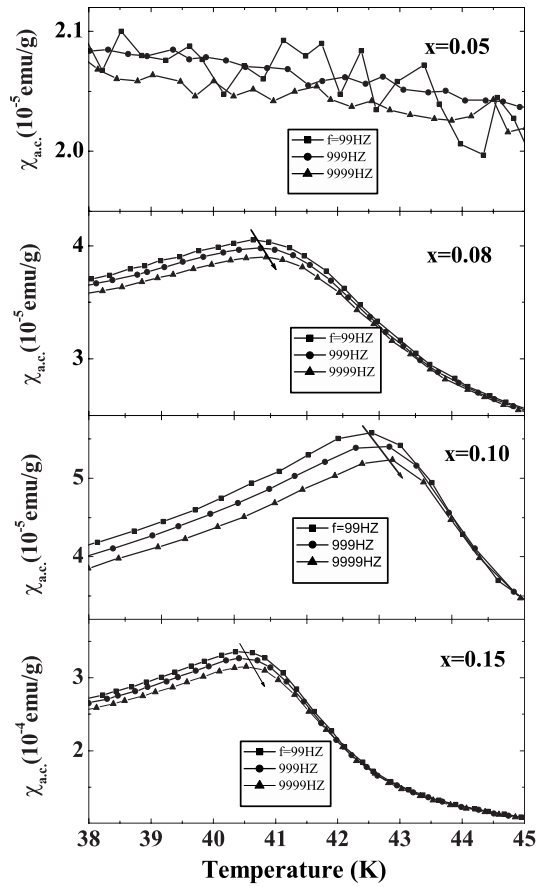


Figure 3. In-plane component of the ac magnetic susceptibility χ_{ac} versus temperature at three frequencies for four typical Mn-rich $\text{YMn}_{1+x}\text{O}_3$ samples ($x = 0.05, 0.08, 0.10,$ and 0.15). All data were collected at an ac field of 10 Oe upon warming under the ZFC condition.

Table 1. The Curie–Weiss temperature θ_{CW} and the effective moment μ_J for $\text{YMn}_{1+x}\text{O}_3$ ($x = 0, 0.05, 0.08, 0.10, 0.12,$ and 0.15), which are obtained by fitting the inverse susceptibility $1/\chi_{dc}$ to the Curie–Weiss law $\chi = C/(T - \theta_{CW})$.

x	0	0.05	0.08	0.10	0.12	0.15
μ_J (μ_B)	4.70	5.12	5.22	5.20	5.31	5.42
θ_{CW} (K)	−330	−461	−542	−530	−513	−507

field of 10 Oe. Figure 3 shows the in-phase component of the ac susceptibility as a function of temperature for $x = 0.05, 0.08, 0.10,$ and 0.15 . A frequency-dependent peak is observed for the samples except for $x = 0.05$. The peak position of the $\chi_{ac} \sim T$ curve (corresponding to the spin freezing temperature T_f) shifts to higher temperature with increasing frequency, and the magnitudes just below it are lower for higher frequencies. Such behaviour is commonly observed in SG systems. Quantitatively, the frequency-dependent shift of the peak position can be obtained from $\delta T_f = \Delta T_f / [T_f \Delta \log(\omega)]$. For SG systems the value of δT_f is in the range 0.004–0.018, while for superparamagnetic systems it is of the order of 0.3–0.5 [13]. For the present samples we find: $\delta T_f = 0.0022$ for $x = 0.08$, $\delta T_f = 0.0035$

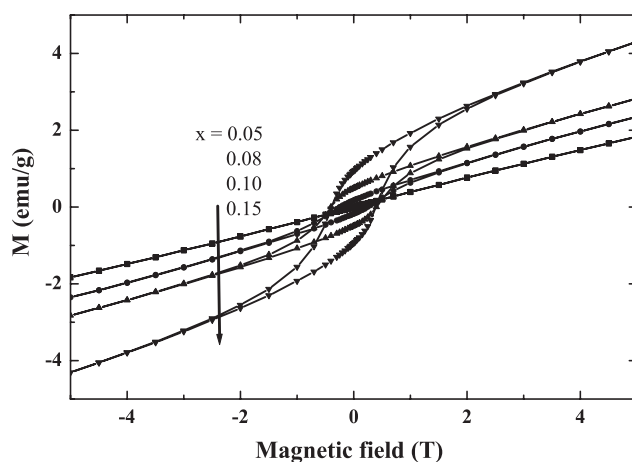


Figure 4. Typical magnetic-field dependence of the magnetization M_H at 5 K under the ZFC condition for four typical Mn-rich $\text{YMn}_{1+x}\text{O}_3$ samples ($x = 0.05, 0.08, 0.10,$ and 0.15). All measurements were carried out by starting at large positive field, sweeping to negative field, and then returning to positive field.

for $x = 0.10$, $\delta T_f = 0.0031$ for $x = 0.12$ and $\delta T_f = 0.0028$ for $x = 0.15$. These values are comparable to but somewhat smaller than those for some previous SG systems. For example, $\delta T_f = 0.005, 0.015,$ and 0.011 were found for CuMn [13], $\text{Ho}_2\text{Mn}_2\text{O}_7$ [14] and $\text{Th}_{0.35}\text{Ba}_{0.30}\text{Sr}_{0.15}\text{Ca}_{0.20}\text{MnO}_3$ [15], respectively.

Figure 4 shows the magnetization of the samples with $x = 0.05, 0.08, 0.10,$ and 0.15 as a function of magnetic field, $M(H)$, under ZFC conditions at $T = 5$ K. In the data of the sample with $x = 0.08$, a obvious hysteresis loop is seen and the magnetization does not saturate even in fields up to 5 T. Such a result is an indication of weak ferromagnetism below T_f and is consistent with a conventional SG system [16, 17]. With the excess Mn concentration increased, both the coercive field H_C and the remanent magnetization M_R become larger. The excess value $x = 0.08$ at which the FM phase occurs is just the value at which the SG phase begins to appear. Therefore, it is reasonable to associate the origin of the SG behaviour with this FM interaction, which may form because of the double-exchange interaction between Mn^{3+} and Mn^{2+} . Such double-exchange interaction between d^{4+} and d^{5+} in the $\text{Mn}^{3+}/\text{Mn}^{2+}$ mixed valence state has been proposed in Zr-doped $\text{Y}_{1-x}\text{Zr}_x\text{MnO}_3$ [11, 18]. It is well known that in a conventional ferromagnet the coercive field H_C is attributed to the blocking of the domain wall motion. Here, the value of H_C , for instance $H_C = 2500$ Oe for the sample with $x = 0.10$, is much larger than those reported for other systems. This may be mainly related to the intrinsic geometric magnetic frustration in this hexagonal system.

For all the compounds, the long-time relaxation of the magnetization was measured in a magnetic field of 100 Oe at 33 K. The curves of normalized magnetization $M(t)/M(0)$ versus time for the samples with $x = 0.05, 0.08, 0.10,$ and 0.15 are shown in figure 5, where $M(0)$ is the magnetization value at the initial measured time. There is a little change with time in the curve for the $x = 0.05$ sample, in which SG behaviour is not observed. However, the magnetization for $x \geq 0.08$ samples increases monotonically with time even after 10^4 s, consistent with an SG behaviour. Such relaxation of magnetization may result from the slow growth of the FM clusters within the AFM matrix. However, the relaxation is very slow, which may be also be attributed to the intrinsic geometric magnetic frustration in the present system. With increasing the excess concentration of Mn, the change of the normalized magnetization

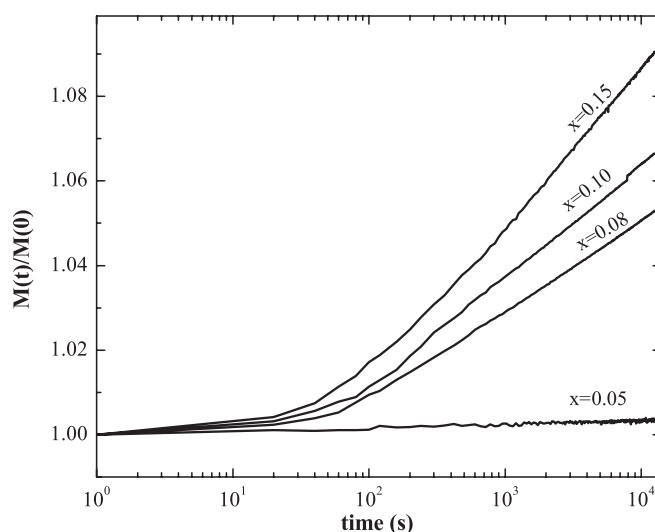


Figure 5. Time dependence of the normalized magnetization $M(t)/M(0)$ at 33 K for four typical Mn-rich $\text{YMn}_{1+x}\text{O}_3$ samples ($x = 0.05, 0.08, 0.10,$ and 0.15), where $M(0)$ is the magnetization value at the initial measured time. The samples were initially cooled down to the measured temperature, and then the magnetic field was applied. After the applied magnetic field was stable, the magnetic data were collected as a function of time. The time at which the first datum was taken is regarded as the initial time.

with time increases noticeably. This may be understood as follows: with increasing the excess of Mn, the degree of geometric magnetic frustration becomes lower and hence results in faster magnetization.

The puzzling ageing phenomena in spin glasses have recently attracted considerable attention [19–22], because they offer a key to understanding the long-debated off-equilibrium dynamic nature of the SG phase. Among these is the most striking ageing behaviour of the TRM. In contrast to the case of orthorhombic $\text{R}_{1-x}\text{A}_x\text{MnO}_3$, the competition between the FM double-exchange interaction and the AFM superexchange interaction in Mn-rich $\text{YMn}_{1.10}\text{O}_3$ is strongly related to its intrinsic geometric magnetic frustration. This special feature should greatly affect the dynamics of the magnetization process and lead in particular to the ageing effect for the SG phase. For these reasons we made careful measurement of the TRM. It took about 700 s to cool the sample down from 60 K through its SG transition temperature to a measured temperature of 33 K in a magnetic field of 30 Oe. After the sample was kept at this state for different waiting times $t_w = 600, 2500, 6300,$ and $10\,000$ s, the magnetic field was rapidly switched off, and the subsequent decays of the TRM were recorded as a function of time. As shown in figure 6, similarly to the case of conventional spin glasses, a larger waiting time t_w results in a slower decay of the TRM. However, the data from the present $\text{YMn}_{1.10}\text{O}_3$ have an essential difference from that of conventional SG systems. For conventional SG systems, the immediate fall-off of the magnetization is usually of the order of 50–90% [23], but such a fall-off in $\text{YMn}_{1.10}\text{O}_3$ is only about 3%. In addition, the decays of the TRM are about one order of magnitude slower than those for conventional spin glasses. These extraordinary properties may have a connection with the intrinsic geometric magnetic frustration in this compound.

One of the methods to clarify the TRM decays is the scaling law suggested by Ocio *et al* [24]. Within the framework of this method, the magnetization scaled by the field-cooled magnetization M/M_{FC} is plotted against an effective waiting time λ/t_w^μ with μ a fitting

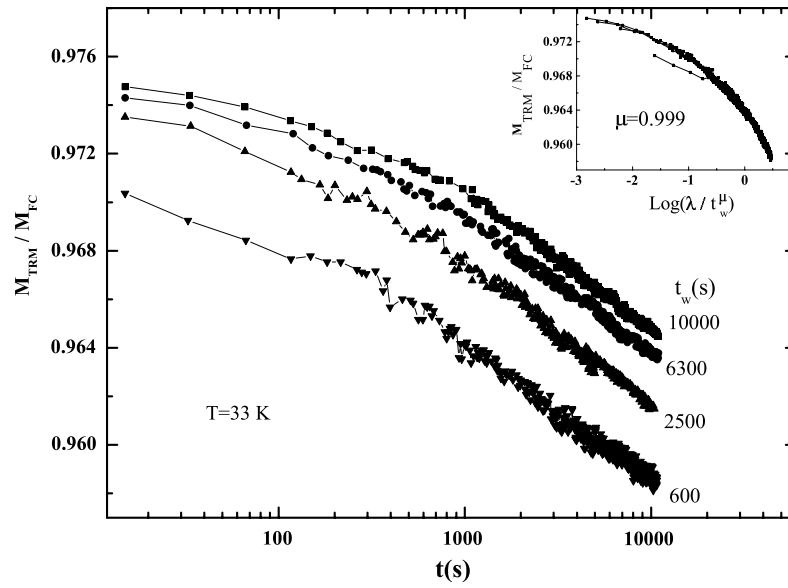


Figure 6. Decays of the thermoremanent magnetization at 33 K, for various values of the waiting time t_w . Inset: the same data are scaled with μ , where $\lambda = \frac{t_w}{1-\mu} \left[\left(1 + \frac{t}{t_w} \right)^{1-\mu} - 1 \right]$ is used.

parameter, where

$$\lambda = \frac{t_w}{1-\mu} \left[\left(1 + \frac{t}{t_w} \right)^{1-\mu} - 1 \right]; \quad \mu < 1 \quad (1)$$

or

$$\lambda = t_w \log \left[1 + \frac{t}{t_w} \right]; \quad \mu = 1. \quad (2)$$

It does not seem that μ has a direct physical meaning, but this is a convenient way of studying TRM decays. $\mu = 0$ corresponds to the case of t_w -independence (no ageing), while $\mu = 1$ would yield a full t/t_w scaling (full ageing). The intermediate values of μ (subageing) correspond to the fact that the apparent age of the SG state, determined from the scaling of the TRM curves, increases more slowly than the waiting time t_w . Full ageing has been predicted within the phenomenological phase-space model based on an SG state with infinite equilibration time [25]. For the TRM on $\text{YMn}_{1.10}\text{O}_3$, the curves for different waiting times $t_w = 2500, 6300,$ and $10\,000$ s can be collapsed onto each other on a $\log(\lambda/t_w^\mu)$ scale with a μ value of 0.999, a perfect scaling (the inset of figure 6). This corresponds to full ageing. One possible reason for the deviation from the perfect scaling for the case of $t_w = 600$ s is that the waiting time is shorter than the cooling time 700 s [26], implying that a waiting time longer than the cooling time may be required to observe full ageing.

It is well known that real SG systems always have a long time in which to approach the equilibrium state, but in fact it is not infinite. As regards the SG state of the present $\text{YMn}_{1.10}\text{O}_3$, the decay of the TRM is at least one order of magnitude slower than that in other samples. That is to say, it must take a longer time to reach the equilibrium state in $\text{YMn}_{1.10}\text{O}_3$. This is the reason why full ageing is easily obtained in $\text{YMn}_{1.10}\text{O}_3$ while subageing is usually found in other samples. The scarce observation of full ageing has been argued with several reasons, one of which is the cooling effect. Recently full ageing has been observed in the SG state of

$\text{Cu}_{0.94}\text{Mn}_{0.06}$ only in the case of a cooling time $t_c^{\text{eff}} < 20$ s [26], which suggests that the cooling rate plays a dominant role in determination of the scaling. In the present work, we find perfect full ageing even when the cooling time t_c^{eff} is as long as 700 s. Therefore it can be concluded that full ageing is an intrinsic nature of an ideal SG state with infinite equilibrium time. Up to now, full ageing has been obtained in two systems: for $\text{Cu}_{0.94}\text{Mn}_{0.06}$ in the case of $t_c^{\text{eff}} < 20$ s, and for $\text{YMn}_{1.10}\text{O}_3$ in the case of $t_c^{\text{eff}} \sim 700$ s. Keeping these two cases together in mind will enable us to find the reason why the cooling effect affects the ageing effect and to solve the long-debated dynamics problem.

4. Summary

We have found an SG state in the Mn-rich hexagonal manganites $\text{YMn}_{1+x}\text{O}_3$ ($0.8 \leq x \leq 0.15$), which is mainly ascribed to the competing magnetic interaction between the FM and AFM states. We have further found full ageing in such an SG state of a typical sample of $\text{YMn}_{1.10}\text{O}_3$ even when the time that the sample takes to reach the measured temperature (33 K) is as long as 700 s. This phenomenon is due to the intrinsic geometric magnetic frustration in the present system.

Acknowledgments

We are grateful to Y M Ni, W W Huang, X L Jing and H Chen for help with experiments. This work is supported by the State Key Program for Basic Research of China and the National Natural Science Foundations.

References

- [1] Zener C 1951 *Phys. Rev.* **82** 403
- [2] De Teresa J M *et al* 1996 *Phys. Rev. Lett.* **76** 3392
- [3] Terai T *et al* 1998 *Phys. Rev. B* **58** 14908
- [4] Dho J, Kim W S and Hur N H 2002 *Phys. Rev. Lett.* **89** 027202
- [5] Pauthenet R and Veyret C 1970 *J. Physique* **31** 65
- [6] Huang Z J, Cao Y, Sun Y Y, Xue Y Y and Chu C W 1997 *Phys. Rev. B* **56** 2623
- [7] Koehler W C, Yakel H L, Wollan E O and Cable J W 1964 *Phys. Lett.* **9** 93
- [8] Fu B *et al* 1994 *J. Mater. Res.* **9** 2645
- [9] Vega D *et al* 2001 *J. Solid State Chem.* **156** 458
- [10] Chen W R *et al* 2005 *Appl. Phys. Lett.* **87** 42508
- [11] Van Aken B B, Bos J-W G, deGroot R A and Palstra T T M 2001 *Phys. Rev. B* **63** 125127
- [12] Martinho H *et al* 2001 *Phys. Rev. B* **64** 024408
- [13] Mydosh J A 1993 *Spin Glasses: An Experimental Introduction* (London: Taylor and Francis)
- [14] Greedan J E *et al* 1996 *Phys. Rev. B* **54** 7189
- [15] Maignan A, Martin C, VanTendeloo G, Hervieu M and Raveau B 1999 *Phys. Rev. B* **60** 15214
- [16] Campbell I A, Senoussi S, Varret F, Teillet J and Hamzic A 1983 *Phys. Rev. Lett.* **50** 1615
- [17] Mukherjee S, Ranganathan R, Anilkumar P S and Joy P A 1996 *Phys. Rev. B* **54** 9267
- [18] Katsufuji T *et al* 2002 *Phys. Rev. B* **66** 134434
- [19] Chamberlin R V, Hardiman M and Orbach R 1983 *J. Appl. Phys.* **52** 1771
- [20] Katsufuji T *et al* 1983 *Phys. Rev. Lett.* **51** 911
- [21] Zotev V S *et al* 2003 *Phys. Rev. B* **67** 184422
- [22] Nordblad P, Svedlindh P, Sandlund L and Lundgren L 1987 *Phys. Lett. A* **120** 475
- [23] Vincent E *et al* 1996 *Preprint cond-mat/9607224*
- [24] Ocio M *et al* 1985 *J. Physique Lett.* **46** 1101
- [25] Bouchaud J P 1992 *J. Physique I* **2** 1705
- [26] Rodriguez G F, Kenning G G and Orbach R 2003 *Phys. Rev. Lett.* **91** 37203